

Target Tracking and Following of a Mobile Robot Using Infrared Sensors

Wei-Shun Yu, Geng-Ping Ren, Chia-Hung Tsai, Youg Jen Wen, and Pei-Chun Lin

*Department of Mechanical Engineering,
National Taiwan University
Taipei, Taiwan*

Corresponding e-mail: peichunlin@ntu.edu.tw

Abstract—An algorithm for target tracking and following on the mobile robot is reported. The target detection, including its direction and distance, is achieved by the low-cost infrared transmitter and receiver pair. Though in the following task the target already performs obstacle avoidance in certain level, a simple but effective obstacle algorithm for the follower is implemented to increase the motion safety level. In addition, the odometry mode is designed as well to deal with the situation while the target is missing. Experimental validation is executed to evaluate the performance the proposed algorithm. With the integrated setup, the follower can track and follow the target in various kinds of complex environment at different designated following distances and speed ranges.

Keywords: human following, infrared sensor, ultrasonic sensor, obstacle avoidance

I. INTRODUCTION

The fast development of the robotics in recent years brings up several new issues regarding the human robot interaction (HRI). How to design a robot which can perform variety of tasks and in the meantime adequately serve and accompany with human in the human environment gradually becomes an important task. Among them, design a mobile platform which can follow the human locomotion is one of the popular topics. In order to achieve this goal, the follower should be capable of detecting the direction and distance from the target, and then it should be capable of moving effectively and safely without any collision with obstacles, thus to follow the target successfully.

Several methods can achieve the target detection or following, and vision is one of the popular methods. For example, using single camera to catch the leg motion of the human target [1], using single camera to catch the infrared signals transmitted from the target [2], using stereo vision to identify the target and obstacle [3], etc. Target tracking achieved by infrared (IR) transmitter and receiver pairs together with fuzzy logic was reported [4]. Inertial sensors was also utilized to compute the target speed and orientation [5]. RFID was adopted to track target by the intensity RF information [6]. In order to get precise motion information, the algorithm which is capable of recognizing people intention by using laser range finder (LRF) was reported [7]. LRF in general is a sensor with high precision, wide detection range, and high reliability. In addition, human tracking by utilizing multiple sensors with fusion scheme was reported as well. For example, fusion of the signals from LRF and vision sensor [8] or fusion of infrared sensors and sonar [9] to

track the target. The successful target tracking includes two subtasks: one is detect the target, and the other one is to perform the adequate locomotion. For the latter one, obstacle avoidance in most scenarios is necessary, and the potential field method is also widely adopted, where the follower was “attracted” to the target and was “pushed away” from the obstacles.

The relation between the target and the follower varies according to the applications. Image in the future you may have an automatic following suitcase, so you no longer need to pull it in travel. Or you may have the automatic following shopping cart, golfing cart, or library chair, which frees your hands for you to enjoy your activities. The suitcase is in general personal belongings, where long-term relationship exists between the target and follower. Thus, in this scenario vision is adequate for this application since (i) the users (i.e., target) is not required to mount additional equipments, which is preferable, and (ii) the required recognition of target by vision system can be trained and learnt through various empirical usages. In contrast, shopping cart, gold cart, or library chair belongs to other owners, so the target and the follower only have short-term relationship. In this situation, the transmitter-receiver based following design is more effective because this method in general doesn't require data training.

Previously, we reported on the design of the target detection module by using the low-cost IR transmitter and receiver pair based on their directional and invisible transmission nature. A primitive following algorithm was also reported. The IR device doesn't need data training, so it is suitable for the target following scenarios where the target and the follower have short-term relationship. Here, with an extensive revision on the usage of the ultrasonic sensors for obstacle avoidance and on the overall algorithm, we report on the robust target tracking and object following of a mobile robot. A simple method is proposed to achieve the obstacle avoidance suitable for the following task. The robot with the proposed algorithm and system integration can track and follow the object with various distance and speed settings as well as can pass and turn in narrow corridors and in complex human environment. In addition, the odometry navigation mode also allows the robot to follow the target path while the signal from it is obstructed.

The paper is organized as follows: Section II briefly reviews the design of the target detection module. Section III presents the locomotion of the follower, and Section IV describes obstacle avoidance algorithm utilized on the follower. Section V reports the results of the

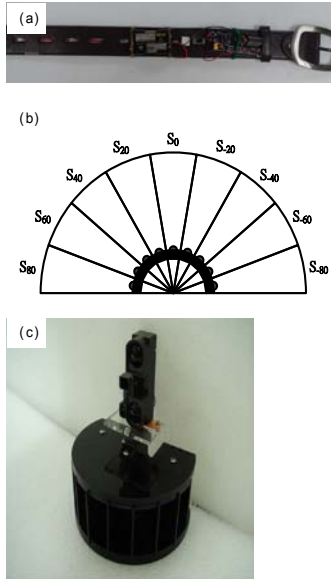


Fig. 1. (a) Photo of the belt with transmitters worn by the target; (b) configuration of nine IR receivers installed inside the semicircle-shaped housing; (c) photo of the target detection device.

experimental evaluation, and Section VI concludes the work.

II. BRIEF REVIEW OF THE TARGET DETECTION MODULE

In order to achieve the target following task, it is necessary for the follower to know the relative position between the target and itself. This information includes two states, the direction and the distance, and more specifically, the position of the target can be represented in the polar coordinates of the coordinate system built on the follower, (δ_o, ℓ_o) , where $\delta = 0$ represents the nominal heading of the follower.

The IR transmitter and receiver are chosen to achieve the direction detection of the target δ_o because the IR light in principle is directional and invisible by the human. The former one and latter one are installed on the target and the follower, respectively. Since the device is intended to be used in the normal environment where lots of other infrared signals may exist, the signal exchanged between the transmitter and receiver are coded according to a specific protocol, which in empirical is done by a commercial transmitter-receiver IC pair. Though the IR light signal itself is directional, the commercial IR transmitter and receivers are usually mounted in the optical lenses to increase the transmitting and receiving angles. To make the signals transmitted from the target omnidirectional, several transmitters are installed and faced different directions. In the human following task demonstrated in this paper, the transmitters are mounted on the belt as shown in Fig. 1(a). In contrast, to prevent the commercial IR receivers to receive the IR signals from unwanted directions, a custom design of the housing of the IR receiver is built as shown in Fig. 1(b).

A bank of nine receivers is adopted to cover the front 180-degree detection range in the final design. In most occasions only one receiver senses the signals from the transmitter, and at most two receivers can sense the signals from the transmitter simultaneously. Assuming

there is no obstacle impeding the light travel from the transmitter to the receiver, the direction of the target δ_o can be computed as:

$$\delta_o = \frac{\sum_i i S_i}{\sum_i S_i}, \quad (1)$$

where

$$i = [80 \ 60 \ 40 \ 20 \ 0 \ -20 \ -40 \ -60 \ -80]$$

representing the physical directions in degree in the follower's coordinate, and

$$S_i = \begin{cases} 1 & \text{triggered} \\ 0 & \text{else} \end{cases} \quad (2)$$

represents the status of the IR receiver. Though 9 terms are summed up in (1), please remind that at most two S_i s are 1 (i.e., receiver triggered), and the others are 0. In addition, the resolution of the δ_o is 10 degree.

Two IR distance sensors are installed on a small RC servo motor to detect the distance between the target and the follower shown in Fig. 1(c). One is for short distance and the other is for long range. After the follower knows the direction of the target, δ_o , the RC servo quickly rotates the IR distance sensors to aim at that direction, so the distance between the target and the follower, ℓ_o , can be obtained. Though the RC servo may not be necessary since the equivalent rotation can be achieved by the motion of the follower itself, by turning the RC rather than the follower itself can avoid the follower performing high frequency rotation or swing motion, so the follower can move in a low frequency smoother trajectory.

In short, the state of the target relative to the follower, (δ_o, ℓ_o) , are obtained. Next, the question lies in how to generate adequate motion of the follower to follow the target.

III. LOCOMOTION OF THE FOLLOWER

During the following motion, the follower is programmed to face the target directly and to follow the target with a designate distance. Thus, at any instant with given (δ_o, ℓ_o) provided by the detection device, the desired setting is $\delta_o^* = 0^\circ$ and $\ell_o^* = \text{constant}$. Generally, the normal social distance between people is about 122-366 cm. Therefore, the designed distance is set to 1m or 2m.

The control goal is to minimize the difference between the current value and the desired one:

$$\begin{cases} \Delta\delta = \delta_o - \delta_o^* \\ \Delta\ell = \ell_o - \ell_o^* \end{cases} \quad (3)$$

The position of the target (δ_o, ℓ_o) changes as the target moves, and the follower updates the new goal and tracks the target. This mode is hereafter referred as the "normal mode". In order to prevent in certain occasions where the detection module does not obtain the new states (i.e., the receivers don't receive any signal from the transmitters), the follower is built in with another "odometry mode" which moves the follower to the last sensed position of the target. During this blind motion, if

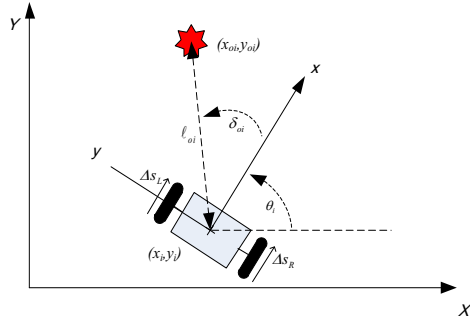


Fig. 2. The maximum forward speed (a) and turning speed (b) versus the errors of target tracking.

the detect module senses the target, the follower shifts back to the normal mode automatically. If no signal from the transmitters appears in between, the follower stops at the last sensed position and enters the “search mode”, where the robot rotates in place to search for the signals from the IR transmitters. Because the IR receivers are installed in the front 180-degree, the rotation of the follower enables the search of the target in all directions around the follower. If the search still fails to locate the target, the follower will stop and wait at the last sensed position. If the target is found, the follower switches back to the normal mode and track the target.

A simple kinematic model is built in the follower to track the motions of the target and the follower. With loss of generality, assume the current state of the follower is $[(x_i, y_i), \theta_i]$, where the first two values and the last one value represents the position and the orientation of the follower at time stamp i , respectively, as shown in Fig. 2. In the two-wheeled differential-drive mobile robot, the incremental movements of the robot in the forward Δs and rotational $\Delta\theta$ directions are

$$\Delta s = \frac{\Delta s_L + \Delta s_R}{2}, \Delta\theta = \frac{\Delta s_L - \Delta s_R}{b}, \quad (4)$$

where Δs_L and Δs_R are the incremental rotations of the left and right wheels in the time stamp i and b is the distance between two wheels. Thus, the state of the robot (i.e., follower) at the next time stamp $i+1$ based on the odometry can be computed as

$$[(x_{i+1}, y_{i+1}), \theta_{i+1}] = [(x_i + \Delta x, y_i + \Delta y), \theta_i + \Delta\theta] \quad (5)$$

where

$$\Delta x = \Delta s \cos(\theta_i + \Delta\theta/2) \text{ and } \Delta y = \Delta s \sin(\theta_i + \Delta\theta/2).$$

In addition, if the state of the target relative to the follower at time stamp i is (δ_{oi}, ℓ_{oi}) , the state of the target in the normal mode can be represented as

$$[(x_{oi+1}, y_{oi+1})] = [(x_{oi} + \ell_{oi} \cos(\theta_i + \delta_{oi}), y_{oi} + \ell_{oi} \sin(\theta_i + \delta_{oi}))]. \quad (6)$$

The states of both target and follower are computed and stored by onboard embedded system in real time. Assuming at time stamp $j+1$ the follower does not acquire new state of the target, the follower enters the

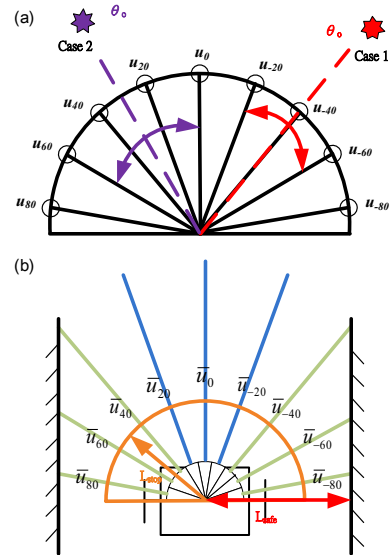


Fig. 3. (a). Configuration of nine ultrasonic range finders installed on the follower; (b) the configuration where the thresholds \bar{u}_j are set up.

odometry mode automatically and treats the state $[(x_{oj}, y_{oj})]$ as the final goal to reach. In the following time stamp i with $i > j$, the dummy target state is computed as

$$\ell_{oi} = \left((x_{oj} - x_i)^2 + (y_{oj} - y_i)^2 \right)^{\frac{1}{2}} + c \ell_o^* \quad (7)$$

$$\delta_{oi} = \text{atan2}(y_{oj} - y_i, x_{oj} - x_i) - \theta_i,$$

where c is the tuned value which gradually increases to 1 while the follower approaches the target. This setting allows the smooth switching from the normal mode to the odometry mode smoothly, and the follower can move to the target but not keep the designate following distance ℓ_o^* . If the follower cannot find the target in the followed time stamp i , it keeps moving to the final goal $[(x_{oj}, y_{oj})]$. Because the positioning of the follower has certain accuracy, the follower is programmed to stop and start the search mode once the follower enters the pre-defined small area centered at the goal $[(x_{oj}, y_{oj})]$. If the target is found at any time stamp $i > j$ before it reaches the goal, the follower automatically shifts back to the normal mode and follows the target according to the newly detected target position.

The follower such as a mobile robot is in general a dynamic system which has certain response characteristic. For the safety reason, the maximum allowable speed is set to confine the motion of the follower. The maximum allowable speed of the robot V_{max} is set as a function of the actual distance. V_{max} increases as ℓ_o increases, to ensure that ℓ_o can be converged to ℓ_o^* . While the actual distance ℓ_o is short, the reduced maximum allowable speed can prevent the follower bumping into the target. The formula is

$$V_{max} = C_{bk} \ell_o, \quad (8)$$

where C_{bk} is a constant roughly determined by the braking performance of the follower.

The motion of the follower basically utilizes speed control strategy. For the forward motion, the quantitative representation of the speed profile versus the following error, $\Delta\ell$, is listed as follows:

$$V = \max(\min(V_o + PID(\ell_o, \ell_o^*), V_{max}), 0), \quad (9)$$

where V represents the forward speed and V_o is the speed of the target, derived from differentiation of ℓ_o . The speed V is adjusted by an ordinary PID control strategy. Equation (9) also reveals that if the following distance is kept at the desired value, the follower also moves at speed V_o , the same as the target. For the turning motion, the quantitative representation of the speed profile versus the following error, $\Delta\ell$, is listed as follows:

$$W = \begin{cases} a_w(\delta_o - \delta_o^*), & (\delta_o - \delta_o^*) > \delta_s \\ W_s, & (\delta_o - \delta_o^*) < \delta_s \end{cases} \quad (10)$$

where W represents the turning speeds, and a_w , δ_s , and W_s are constants. Because the resolution of direction detection δ_o is 10 degree, the PID controller is not effective. Instead, a simple proportional control is utilized. For small error $\Delta\delta < \delta_s = 15^\circ$, a smaller value W_s is set to prevent overcorrection owing to the slow dynamic response of the robot. For safety reason, equation (10) also constrains the follower to move backward because no ultrasonic sensor senses the back side of the follower.

In the empirical evaluation where the follower is a two-wheeled differential-drive mobile robot, the forward and turning speed can further be converted to the forward speeds of the left and right wheels, V_L and V_R ,

$$\begin{cases} V_L = V + bW/2 \\ V_R = V - bW/2 \end{cases} \quad (11)$$

The rotation speeds of the left and the right wheels, $\dot{\phi}_L$ and $\dot{\phi}_R$, can then be calculated as

$$\begin{cases} \dot{\phi}_L = \frac{V_L}{R} \\ \dot{\phi}_R = \frac{V_R}{R} \end{cases}, \quad (12)$$

where R is the radius of the wheel.

IV. OBSTACLE AVOIDANCE

If the follower tails the target very closely, the motion of the follower can be programmed to directly follow the “movable” target point (i.e., a tracking problem). In this case the obstacle avoidance capability in the follower is not necessary as long as the target can find an accessible path and avoid the obstacles successfully. In this case, actually it is the target itself to perform the obstacle avoidance.

In general following tasks where certain distance exists between the target and the follower, the capability of obstacle avoidance in the follower is crucial. For example, in the case of human following where the comfortable distance for human to be tailed is at least 1 meter, it is hard to guarantee that the space between the human and the follower is clear at all time. Thus, in this section

the motion of the follower with obstacle avoidance capability is described.

As reported in, nine ultrasonic range finders are installed on the follower to cover the front 180-degree environment sensing capability as shown in Fig. 3(a). The installation and alignment of the ultrasonic range finders are similar to that of the IR receivers, equally distributed on the semicircle. Thus, the difference of the main sensing direction between the consecutive sensors is 20 degree. The ultrasonic range finder itself has ~45 degree receiving cone, so in current arrangement the sensing areas have some overlap to make sure the front area are sensed thoroughly. Assume u_j is the distance of the obstacle measured by the sensor, where the notation $j = [80 \ 60 \ 40 \ 20 \ 0 \ -20 \ -40 \ -60 \ -80]$ indicates the physical sensing directions of the sensors, similar to the notations of the IR receivers shown in the section II.

Nine threshold \bar{u}_j s are defined as the safety measure of the follower’s motion. Because the follower faces the target most of the time, the defined thresholds of the six range finders on both sides are mainly determined by the geometrical configuration of the follower relative to the imaginary side wall as shown in Fig. 3(b). Here L_{safe} is set to 55cm and the \bar{u}_j s are calculated as $\bar{u}_j = L_{safe}/\cos(90 - abs(j))$, where $j = \pm 40, \pm 60$, and ± 80 . Because the combined sensed range of the three front sensors is wider than the width of the follower, the \bar{u}_j s of these three are treated as the judgment whether the follower can go straight forward or not. Empirically the value is set to $\bar{u}_j = 75$ cm, $j = 0, \pm 20$. In addition, when the sensed u_j is less than $L_{stop} = 37.5$ cm, the follower stops immediately to avoid any potential collision.

A function $f_j(u_j)$ is defined to represent the obstacle status around the follower:

$$f_j(u_j) = \begin{cases} 1 & \text{if } u_j \leq \bar{u}_j \\ 0 & \text{else} \end{cases}, \quad (13)$$

where the value 1 indicates that the robot is too close to the obstacle in the j direction. The value 0 indicates no obstacle in that direction. Because the combined sensed range of three consecutive sensors is wider than the width of the follower, the follower can move safely toward the center of the three consecutive sensors which shows 0. Following that logic, the feasible following direction δ_b with obstacle avoidance (hereafter referred to as front obstacle avoidance) can be described as

$$\begin{cases} \delta_b = \delta_o & \text{if } \sum_j f_j(u_j) = 0 \quad j = \delta_o, \delta_o \pm 20 \\ \delta_b = \tilde{\delta}_o & \text{if } \sum_j f_j(u_j) = 0 \quad j = \tilde{\delta}_o, \tilde{\delta}_o \pm 20 \quad \min\|\delta_o - \delta_o\| \end{cases} \quad (14)$$

if the direction of the target θ_o is derived to be the same as one of the number j (i.e., 0, 20, 40, ...), as the case 1 shown in Fig. 3(a). If the derived θ_o is derived to be in between the number j s (ex, 10, 30, ...), the criteria is

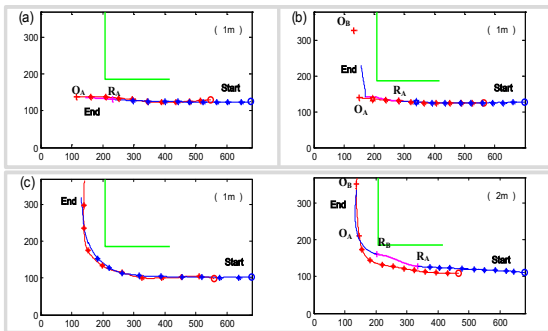


Fig. 6. Trajectories of the target (red line) and the follower (blue line) in various scenarios viewing from the ceiling (top view). Walls/obstacles are shown in green color and the designated following distance (1m or 2m) is shown at the upper right corner of each scenario. When the robot is operated in the odometry mode, the trajectory is marked in pink color. (a) odometry mode and stop; (b) odometry mode and then back to normal mode; (c) right angle turn

the target and the follower as the markers during the experiments, which ease the followed post processing in Matlab to extract the positions of the markers from a sequence of images. The results are shown in Fig 6 and Fig 7, where the red line and blue line represent the trajectories of the target and follower, respectively. The special legends marked on both lines indicate the positions extracted from the same image, and this information provides the relative position between the target and the follower at several different time stamps.

Figure 6(a) plots the trajectories of the target and the follower where the follower loses the signal from the target (intentionally turns off the transmitter) at point R_A . The follower enters the odometry model and successfully moves to the last target position O_A within certain error range. It then performs the search mode (i.e., turning in place), but because no target is found, the follower rests around the last target position O_A . In Fig. 6(b), the follower also goes through normal mode, odometry mode, and then search mode by the similar setting (intentionally turns off the transmitter). At certain moment after the transmitter is intentionally back on, the follower finds the target at O_B and moves directly toward the target. Figure 6 (c) to (e) compare the performance of the following with different designated following distances. In the simple turning motion shown in Fig. 6(c)-1m, the follower can track the target well with smooth trajectory close to that of the target. For the case in Fig. 6(c)-2m, because of the longer following distance, at certain time period right after the turning of the target, the follower loses the signals from the target and enters the odometry mode (pink line segment, between R_A and R_B), but it then recovers back to the normal mode at the later moment before it reaches the target point O_A . Thus, the follower goes back to the normal mode from the search mode, not entering the search mode. Comparing to Fig. 6(b) which has a sharp turning owing to the turning in place in search mode, the trajectory shown in Fig. 6(c)-2m has a smoother trajectory.

VI. CONCLUSION

We report on the target tracking and following algorithm based on the developed IR-based target detection

module. With given target direction and distance, the follower generates the adequate motion with obstacle avoidance to track the target. The follower can also detect the speed of the target and follows it accordingly. If the signal from the target is lost, the follower switches to the odometry mode to move to the last target position and search for the target. As long as the target is found, the follower automatically switches back to the normal mode and keeps following task. The algorithm is experimentally evaluated and is proved functional.

We are current in the process of developing a more sophisticated algorithm which can perform target following with faster following speed and in a complicate and wide range of environment setup.

VII. ACKNOWLEDGMENT

The authors gratefully thank the National Instruments Taiwan Branch for their kindly support of technical consulting.

REFERENCES

- [1] N. Tsuda, S. Harimoto, T. Saitoh, and R. Konishi, "Mobile robot with following and returning mode," in *The 18th IEEE International Symposium on Robot and Human Interactive Communication (RO-MAN)* 2009, pp. 933-938.
- [2] Y. Nagumo and A. Ohya, "Human following behavior of an autonomous mobile robot using light-emitting device," in *IEEE International Workshop on Robot and Human Interactive Communication (RO-MAN)* 2001, pp. 225-230.
- [3] C.-H. Chao, B.-Y. Hsueh, M.-Y. Hsiao, S.-H. Tsai, and T.-H. Li, "Real-time target tracking and obstacle avoidance for mobile robots using two cameras," in *ICROS-SICE International Joint Conference*, 2009, pp. 4347-4352.
- [4] T. H. S. Li, C. Shih-Jie, and T. Wei, "Fuzzy target tracking control of autonomous mobile robots by using infrared sensors," *Fuzzy Systems, IEEE Transactions on*, vol. 12, pp. 491-501, 2004.
- [5] S. Bosch, M. Marin-Perianu, R. Marin-Perianu, H. Scholten, and P. Havinga, "Follow me! mobile team coordination in wireless sensor and actuator networks," in *IEEE International Conference on Pervasive Computing and Communications (PerCom)* 2009, pp. 1-11.
- [6] K. Myungsik, C. Nak Young, A. Hyo-Sung, and Y. Wonpil, "RFID-enabled target tracking and following with a mobile robot using direction finding antennas," in *IEEE International Conference on Automation Science and Engineering (CASE)*, 2007, pp. 1014-1019.
- [7] K. Seongyong and K. Dong-Soo, "Recognizing human intentional actions from the relative movements between human and robot," in *IEEE International Symposium on Robot and Human Interactive Communication (RO-MAN)* 2009, pp. 939-944.
- [8] R. C. Luo, C. Nai-Wen, L. Shih-Chi, and W. Shih-Chiang, "Human tracking and following using sensor fusion approach for mobile assistive companion robot," in *Annual Conference of the IEEE Industrial Electronics Society (IECON)*, 2009, pp. 2235-2240.
- [9] A. Korodi, A. Cedrean, L. Banita, and C. Volosencu, "Aspects regarding the object following control procedure for wheeled mobile robots," *WSEAS Transactions on Systems and Control*, vol. 3, pp. 537-546, 2008.